2 https://ascelibrary.org/doi/abs/10.1061/%28ASCE%29AE.1943-5568.0000418 3 4 Tessellated Structural-Architectural Systems: A Concept for Efficient Construction, 5 Repair, and Disassembly 6 Brandon E Ross (corresponding author): Cottingham Associate Professor, Glenn Department of Civil Engineering, 109 Lowry Hall, Clemson University, Clemson, SC 29634-0911. 7 bross2@clemson.edu 8 9 Cancan Yang: Assistant Professor, Department of Civil Engineering, McMaster University, 10 Hamilton, ON, Canada. cancanyang@mcmcaster.ca 11 Michael Carlos Barrios Kleiss: Associate Professor of Architecture, Structures & Computation & Watt Family Innovation Center Faculty Fellow, School of Architecture, Lee Hall 3-123, 12 Clemson University, Clemson, SC 29634-0911. crbh@clemson.edu 13 14 Pinar Okumus: Associate Professor, Department of Civil, Structural and Environmental 15 Engineering, 222 Ketter Hall, University at Buffalo, Buffalo, NY 14260. pinaroku@buffalo.edu 16 Negar Elhami Khorasani: Assistant Professor, Department of Civil, Structural and Environmental Engineering, 136 Ketter Hall, University at Buffalo, Buffalo, NY 14260. 17 negarkho@buffalo.edu 18 19 20 **Abstract** 21 This paper introduces a tessellated structural-architectural (TeSA) wall system concept with the potential for improving both resilience and sustainability of the built environment. Resilience 22 23 requires fast recovery and restoration of building functionality after an extreme event, while 24 sustainability seeks designs that facilitate building adaptability and reuse for long term 25 occupancy. TeSA wall systems are comprised of individual interchangeable tile segments which 26 are arranged in tessellated (repetitive) patterns. TeSA walls provide a resilient and sustainable 27 solution wherein tiles can be prefabricated, reconfigured, disassembled, and reused during the

Manuscript accepted by the ASCE Journal of Architectural Engineering May 2020

lifetime of a structure. This paper introduces the TeSA concept through preliminary physical and analytical studies. The physical test involved a beam made of interlocking tessellated acrylic tiles which was loaded to failure. The analytical study featured two reinforced concrete TeSA shear walls under lateral loading. The physical test showed that damage can be localized within individual tiles which can be replaced to restore loadbearing capacity. The analyses showed that TeSA shear walls can provide ductility and localized damage in individual tiles.

Recommendations for advancing the TeSA toward implementation are also discussed.

Author keywords: Tessellations, structural-architectural wall systems, topological interlocking, non-interlocking, shear wall, localized damage

Introduction

This paper describes an integrated structural-architectural system concept which utilizes tessellated elements (patterns arrangement from similar and/or repetitive elements, Fig 1) to produce buildings that can be efficiently constructed, repaired, reconfigured, and deconstructed. In particular, tessellated structural-architectural (TeSA) wall systems capable of resisting inplane vertical and lateral loads while also creating aesthetically compelling patterns are described. Although tessellations have previously been used in buildings for architectural purposes, their use as structural-architectural systems has been limited. This paper provides an introduction to TeSA wall systems and investigates their potential benefits as repairable systems that are capable of localized damage. TeSA wall systems are currently in the conceptual stages of development. Recommendations for further development are also discussed.

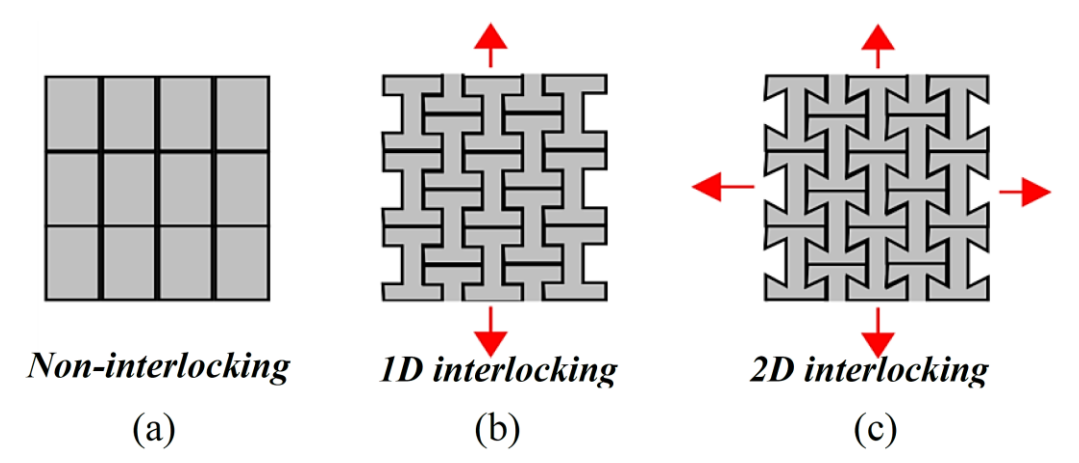


Fig. 1. (a) Example of non-interlocking tessellation, (b) Example of 1D interlocking, separation is prevented in one direction, (c) Example of 2D-interlocking, separation is prevented in two directions.

Examples of TeSA patterns are shown in Fig 2. One potential benefit of TeSA systems is their ability to localize structural damage. Localized damage occurs because of the segmented nature

of individual elements in a TeSA wall. When subject to a sufficiently large load, cracking will occur locally in one or more elements; however, cracking is arrested when it reaches a free edge. Cracks cannot propagate as they would in a solid (i.e. non-segmented) structure, and damage is thus localized to individual elements. In theory, damaged segments can be replaced after an extreme event and the building can be returned to its pre-damaged state. This feature of TeSA may contribute to reparability and rapid recovery.

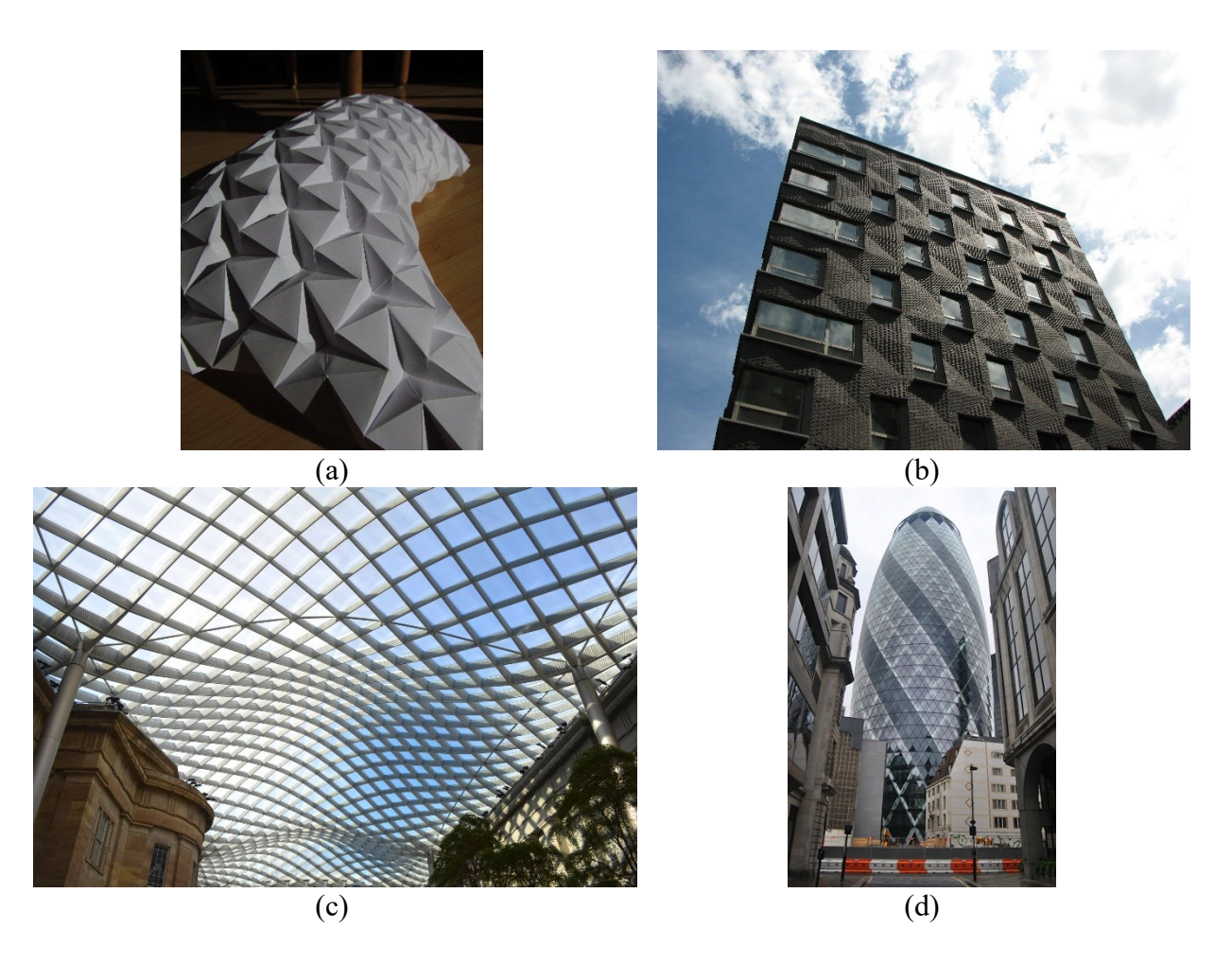


Fig. 2. (a) Example of a 3D tessellation (Adami 2012), (b) non-structural tessellated façade of the Mulbery House with prefabricated tiles (Manning 2009), (c) tessellated roof (Evanson 2013), (d) tessellated exterior frame (Steve 2012)

Construction efficiency and visual appeal are also potential benefits of TeSA systems. The tessellated exterior facade of the Mulberry House in NYC (Fig 2 (b)), while not part of the primary structural system, demonstrates these benefits. The facade is composed of similar precast concrete L-shaped segments that are offset floor-to-floor to create alternating window locations for aesthetic design and flexibility. Surface treatments placed on the exterior faces of the panels add to the visual interest from the tessellated pattern. Individual segments are similar, if not identical, and were produced in a precast facility with repetitive use of forms, details, and processes. Efficiency was created through repetition and through minimizing the number of "one off" conditions and pieces. Thus, the Mulberry House facade makes a striking visual statement while also being efficient to fabricate and install. Development and implementation of TeSA wall systems may contribute to one of the Grand Challenges for Engineering identified by the National Academy of Engineering: restoring and improving urban infrastructure (Perry et al. 2008). Because TeSA systems are built of repetitive discrete segments, they are well-suited for prefabrication, automated construction, reconfiguration, disassembly, and reuse. The preliminary research presented in this paper demonstrates that TeSA systems have the ability to localize structural damage during extreme events to individual tiles within a pattern, while simultaneously providing alternate load paths for ductility. Damaged tiles in TeSA walls can be repaired or replaced after extreme events allowing TeSA buildings to be quickly reoccupied. It is also theoretically possible to design TeSA walls with "weak" tiles at pre-selected locations to control localized damage where needed or desired. In these ways, TeSA systems may contribute to resilience through rapid repair and reoccupation, and to sustainability through reuse and adaptability.

68

69

70

71

72

73

74

75

76

77

78

79

80

81

82

83

84

85

86

87

88

This paper is presented in five parts. First, an overview is presented on the geometric background of tessellations. Previous research on tessellations in materials and structures is discussed. Second, a proof-of-concept experiment is presented. The experiment utilized a small beam comprised of tessellated acrylic segments, which is loaded to failure and then repaired and reloaded. Third, a numerical investigation of TeSA walls under lateral loading is presented. Nonlinear finite element analyses are conducted to investigate the strength, ductility, and damage localization of alternative TeSA patterns and details. Fourth research needs and the hurdles preventing widespread implementation are discussed. Finally, a summary of the paper and recommendations on the path forward are provided.

Background

Tessellations: Geometry

From the field of Geometry, a tessellation in the plane (2D) is an arrangement of closed convex regular polygons (shapes) that fit together in a repeating manner creating a pattern. In this definition a regular polygon is an n-sided closed shape in which all sides are the same length, have the same value for all internal angles and are at the same distance from a common point (center). The geometry and characterization of tessellations is an expansive topic and the focus of many books and articles (e.g. Critchlow 1970, Magnus 1974, Chavey 1989) which are beyond the scope of this paper. However, few basic concepts are mentioned here by way of context and background for the rest of the paper.

In mathematics, plane tessellations (also 2D tessellations) are classified as regular, semi-regular and demi-regular. A regular tessellation is an arrangement composed of regular polygons of the same shape and size that creates a pattern with no gaps or overlaps between them (Fig. 3a).

Semi-regular tessellations are made with two or more regular polygons (Fig. 3b), also forming a

pattern with no gaps or overlaps. Demi-regular tessellations (Fig. 3c) are more problematic to define as experts in the field do not agree on a unified definition. Some experts argue that demi-regular are a combination of regular and semi-regular, while others define them as having several classes of transformations leading to a seemingly infinite number of possibilities.

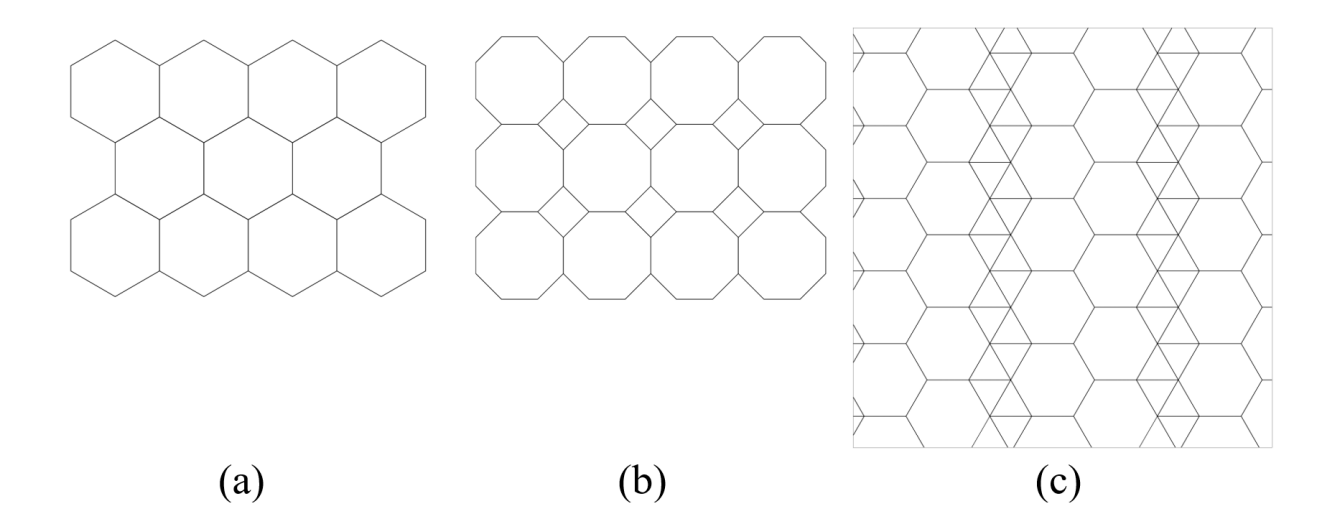


Fig. 3. (a) Regular Tessellation, (b) Semi-regular Tessellation, and (c) Demi-regular Tessellation.

Architects use a less dogmatic definition of a tessellation to include patterns formed by non-regular polygons, that in some cases allow the occurrence of gaps and overlaps in the pattern. This paper will use the architect's loose definition of a tessellation as an arrangement of one or more types of polygons (shapes), that form a distinguishable and repeating pattern where gaps and overlaps may occur. This allows the inclusion of some useful shapes and patterns that otherwise will not be considered as tessellations from the strict mathematical definition, such as the ones in figure 1b and 1c, but that are useful for architectural and engineering purposes. The architect's definition of tessellations allows the inclusion of the 1D and 2D interlocking patterns shown in Figures 1b and 1c.

Out of these many patterns that can be created some lend themselves to architectural and structural use. This paper investigates some of these patterns that can be constructed in large scale for architecturally appealing and structurally resilient buildings. Tessellations: Architecture Tessellations have been used in architecture since ancient Rome. Early precedents are found in Greek pottery meanders and a few building decorations (Knight 1986). They flourished during the mid-ages as shown in the decorative patterns of the Alhambra palace in Granada, Spain. But with a few exceptions, such as the dome roof of the Pantheon in Rome built between 27 BC and 14 AD (Moore 1995a; Moore 1995b), tessellations were used predominantly for decoration and not for structural purposes (Knight 1995). Recent use of tessellations in architecture includes façade systems for environmental controls. Two notable examples are the award winning Institut du Monde Arab (Arab World Institute) designed by Architecture Studio in collaboration with French architect Jean Nouvel in 1981-87 (Fig 4 (a)) and the more recent Al Bahar towers in Abu Dhabi designed by AEDAS studio in collaboration with ARUP (Fig 4 (b)). In both cases, the geometry of the façade uses an Islamic inspired geometry for control of natural light. Another interesting example is the recently completed *Mulberry House*, a 13-story mixed-use residential and commercial building located in New York City (Fig 2 (b)). Notable for its use of brick embedded in precast concrete panels, the building is distinguished by the highly articulated façade showcasing intricate use of brick tiles, a requirement for buildings in its historical neighborhood. The arrangement of the precast concrete panels forms an aesthetically dynamic enclosure. Even though they are pre-manufactured from one single mold, the arrangement of the

130

131

132

133

134

135

136

137

138

139

140

141

142

143

144

145

146

147

148

149

150

151

152

panels is staggered and creates undulations on the building's exterior. However, this tessellated

façade panel system is only a building enclosure and not part of the structural system. The proposed TeSA concept in this paper will combine the architectural appeal demonstrated by the Mulberry House with the technical benefits of tessellated structures as described in the next section.

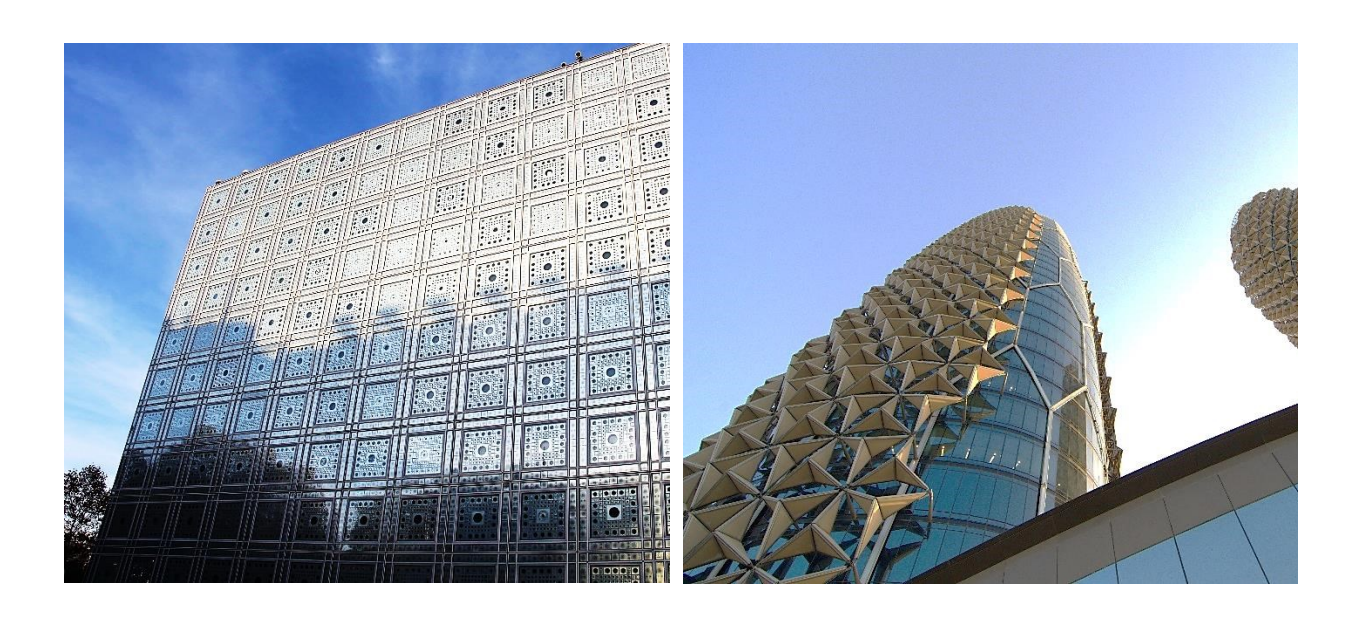


Fig. 4. Tessellations controlling natural light: (a) Arab World Institute (fee-ach 2006) (b) Al Bahar Towers (Epsilon 2013).

(b)

Tessellations: Structures

(a)

Structural tessellations can be characterized as either non-interlocking or topologically interlocking patterns (Fig 1). If a tessellated pattern is considered as a 2D structure, then topologically interlocking elements can be defined as patterns that maintain structural integrity without the need for binders or other tensile connections between the tiles. Removal of tiles in an interlocking tessellation is prevented by contact with neighboring tiles (Estrin et al. 2004).

Brick patterns such as running bond are non-interlocking tessellations and require tensile connections such as mortar and reinforcing bars between the bricks to maintain structural integrity. Such patterns are ubiquitous, well-understood, and are not discussed in this paper. In contrast, topologically-interlocking structures (Fig 1 (b), (c)) are relatively uncommon and the application of this class of structures at the building scale has received little attention. Topologically-interlocking building structures were proposed as early as the 17th century by French Architect Joseph Abeille (Fleury 2009). The Abeille Vault is a 2D floor structure comprised of interlocking 3D blocks that can support out-of-plane vertical loads. It is a tessellation because it utilizes repetitive individual blocks. In the 1980s, Glickman (Glickman 1984) created "G-blocks", a tessellated system of pavement blocks which rely on interlocking tetrahedra. Structures such as the Abeille Vault and G-block system require boundaries capable of restraining lateral movement similar to how buttresses are used to support arches (Khandelwal 2013). In contrast, the TeSA systems in this paper do not require buttresses or supports beyond those required for traditional shear walls. Perhaps the most intriguing feature of topologically-interlocking structures is that they can have high damage tolerance relative to similarly sized solid structures. This occurs because cracking in a single element may be arrested when it reaches a free edge. Cracks cannot propagate as they would in a solid (i.e. non-segmented) structure, and damage is thus localized to individual elements. Experimental examples of this behavior at small-scales have been reported (Estrin et al. 2004; Molotnikov et al. 2007), but this feature has not been researched at the scale of civil engineering structures. Another technical benefit of topologically-interlocking structures is re-manufacturability. Mather et al. (2012) modeled initial damage and the effects of repaired tiles on small-scale structures.

166

167

168

169

170

171

172

173

174

175

176

177

178

179

180

181

182

183

184

185

186

187

building-scale structures. Other work on topologically-interlocking structures have described occurrences in biological structures (Dunlop and Brechet 2009; Krauss et al. 2009), creation of negative-stiffness hysteretic devices (Estrin et al. 2004; Schaare et al. 2008), finite element and discrete element formulations for small-scale modeling (Brugger et al. 2009), application to 3D printing of concrete (Zareiyan and Khoshnevis 2017), and application to brick masonry (Rezaee Javan et al. 2017). While the technical features of tessellated structures - particularly topologicalinterlocking structures - have been established at small scales, applications at the building scale have received limited attention. Thus, the focus of this paper is the extension of non- and topologically interlocking tessellations to building structures. When tessellations have been used previously in building structures, they have primarily been used in frames (Fig 2 (d)). Diagrids are one example of non-interlocking, mechanically connected, tessellated frame structures that have been utilized in buildings (Moon et al. 2007). While tessellated frame structures can be elegant and efficient, their design intent is not necessarily resilience or reparability. In contrast to tessellated frames, TeSA systems feature tessellated structures built of repetitive tile elements. **Proof of Concept Physical Test** A simple physical experiment was conducted to demonstrate the primary technical benefits of tessellated structures, namely localization of damage and repair potential. A small acrylic glass beam was built of 2D topologically-interlocking tiles (Fig 5). The choice of material and

The TeSA concept extends the reparability observed in small-scale tests and simulations to

189

190

191

192

193

194

195

196

197

198

199

200

201

202

203

204

205

206

207

208

209

210

211

tessellation pattern was made for practical and aesthetic reasons. The individual acrylic pieces

were relatively easy and inexpensive to fabricate. An architecture student designed the pattern to

be 2D interlocking and to have the subjective quality of being visually interesting. The beam was simply supported and subjected to displacement-controlled loading. Displacement was increased until the beam failed.



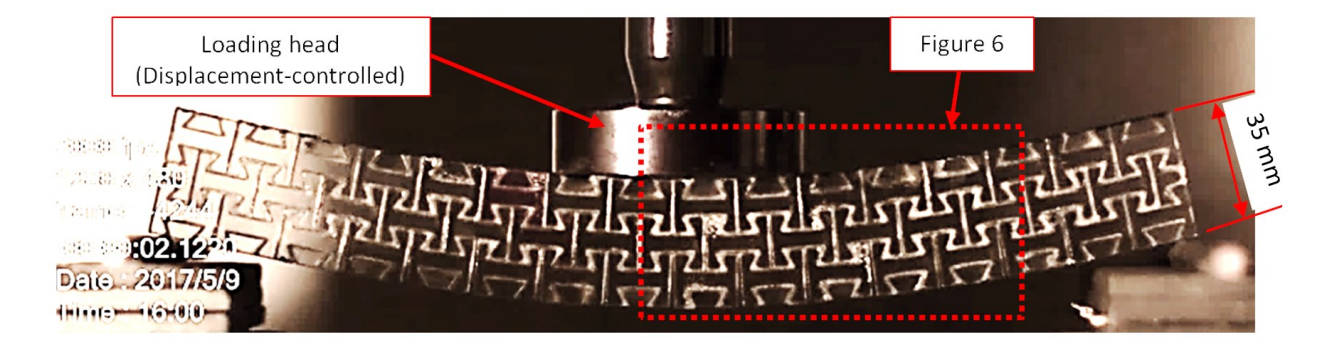
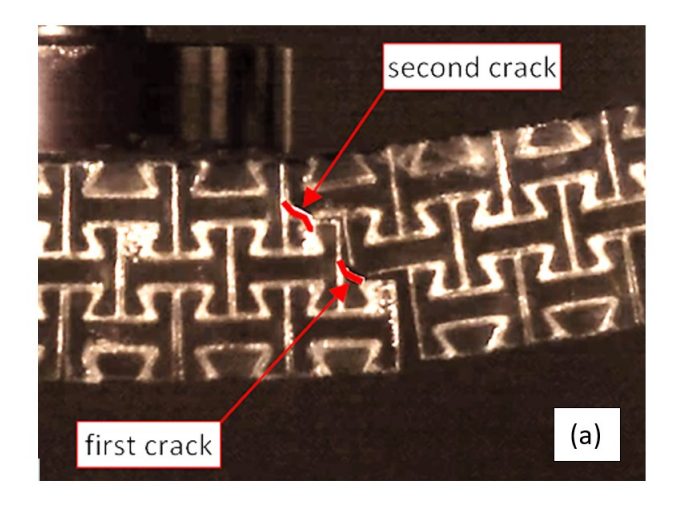


Fig. 5. Beam comprised of topologically interlocking tessellated tiles.

As expected in an interlocking tessellation, damaged was localized in individual tiles. Using high-speed video, it was observed that the damage initiated in one of the mid-row tiles near the loading head Fig 6). The first crack started at the reentrant corner of a tile. The failure is attributed to a stress concentration forming at that location due to the tile geometry and due to flexural-tension action in the beam which resulted in the corner being "pried" open. A second crack formed immediately following the first, in a top-row tile near the edge of the loading head (Fig 6). The entire beam collapsed after the second crack occurred because the beam with only three layers of tiles had no alternative load paths to support the flexural action. After the initial test, the damaged tiles were removed and replaced with undamaged tiles and the beam was loaded again. The maximum load and displacement of the repaired beam was 55 N (12 pounds) and 17 mm (0.67 in). Stiffness and strength of the repaired beam were similar to that of the original.



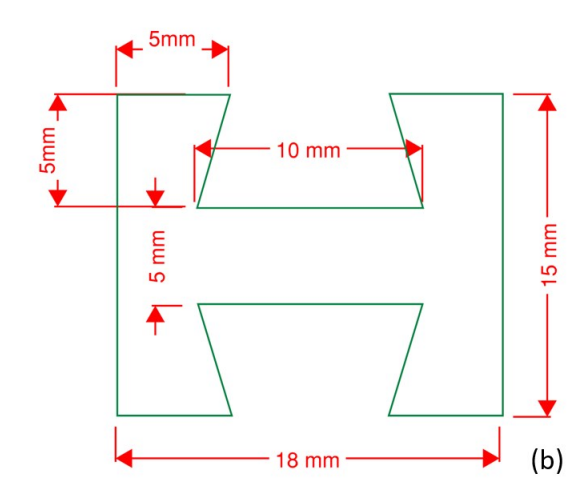


Fig. 6. Cracking identified from high-speed video (a) and approximate tile geometry (b).

Load-displacement behavior in the original and repaired beams were linear-elastic until failure. Although displacement-based load control was used in the experiment, the fracture energy released by the first damaged tile could not be absorbed in alternative load paths and the entire structure failed in a brittle manner. This result is attributed to the brittle nature of the acrylic material and the low number of tile rows (three). As demonstrated by the analytical program presented in the next section, load redistribution and ductility are possible in tessellated structures that include ductile materials and larger arrays of segments.

This simple experiment demonstrated two key features of interlocking tessellated structures. First, damage can be localized within individual segments. Second, damaged segments can be replaced and structural capacity can be restored. Together, these features can be exploited to create resilient, readily repairable systems of prefabricated and replicated segments. Significant effort is no doubt required to take this concept from the simple experiment to realization in building-scale structures. The remainder of this paper focuses on how the benefits of interlocking tessellations can be realized at the building-scale.

Analytical Program

Walls

Behavior of reinforced concrete shear walls under lateral loading was investigated analytically using finite element modeling. The analyses were conducted for 1) a wall with L-shaped, non-interlocking tessellations, and 2) a wall with 2D topologically interlocking tessellations.

Tessellation patterns and dimensions of the two walls are shown in Fig 7. The walls were 152.4-mm (6-in.) thick. The non-interlocking wall with L-shaped tessellations was inspired by the non-structural façade of the Mulberry House (SHoP Architects n.d.) located in New York, NY. This wall model had mild-reinforcement connectors between individual tiles and at the tile-foundation interface. These connectors were made of U-shaped, No. 9 mild steel rebars and acted as replaceable sacrificial fuses. Unbonded vertical post-tensioning strands provided self-centering in addition to connecting tiles to each other and to the foundation. There were no mechanical connectors or post-tensioning strands for the topologically interlocking wall. All translational degrees of freedom at wall base were restrained, creating a fixed support at wall base.

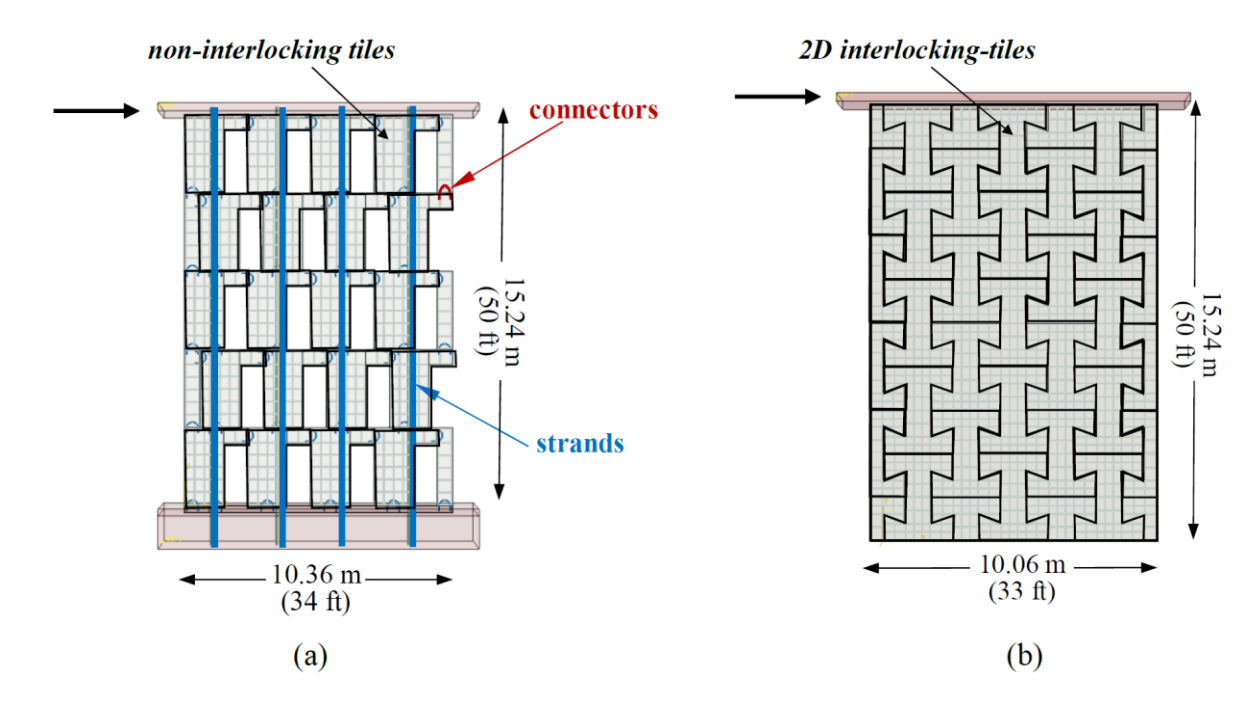


Fig. 7. (a) Non-interlocking and (b) topologically-interlocking walls studied using finite element analyses.

Finite Element Model Features

The walls were modeled using the commercial finite element modeling software, Abaqus (Dassault Systèmes Simulia Corporation 2016). The models featured material nonlinearity to capture post-yield behavior. A lateral displacement was applied on top of the wall, to create load-displacement curves up to 1.7% drift ratio. The out-of-plane displacement was restrained at wall top, where lateral load was applied.

The tiles were taken to be concrete and were modeled using first order, 8-node, 3D hexahedral elements (C3D8R). No external out-of-plane restraints were applied on the tiles. Tile mild reinforcement and connectors between tiles (non-interlocking wall only), were modeled using 2-node linear 3-D truss elements (T3D2 in Abaqus). Connectors between tiles can restrain both in-plane and out-of-plane displacements, if there is any. The unbonded post-tensioning strands were

modeled using 2-node linear beam elements (B31 in Abagus). Mild reinforcement and connectors were embedded into hexahedral elements using a node-tie constraint. The tile reinforcement ratios in the longitudinal and transverse directions (loading direction) were 0.31%, and 0.02%, respectively. A short length of post-tensioning strands was embedded into the top of the wall and the foundation to simulate the anchorages. The non-interlocking wall (Fig 7 a) utilized four groups of strands in the vertical direction. Each group consisted of ten 15.2-mm (0.6-in.) diameter, 7-wire, 270-ksi ultimate strength, low-relaxation strands. Each strand was initially post-tensioned to 89 kN (20 kips) or 34% of the ultimate strength of the strands. The axial force on the tiles due to post-tension corresponds to approximately 15% of the axial capacity of the wall. Interaction between tiles was simulated by surface-to-surface hard contact that allowed gap opening. Shear-slip is considered undesirable for TeSA walls because it is unpredictable. Shear-slip was intentionally minimized by using a friction coefficient of 1.0 for hardened and intentionally roughened concrete (ACI 318 2014). In practice, surface roughening, materials with high friction coefficient, grout, or special connectors between tiles can be used to minimize shear-slip. Tiles were assumed braced against out of plane displacements at the base and top of the walls. In practice, out of plane restraint can be provided by designing tiles to span vertically floor-to-floor so that they are braced by floor diaphragms.

Material Properties

278

279

280

281

282

283

284

285

286

287

288

289

290

291

292

293

294

295

296

297

298

299

300

Concrete material properties were defined using the damaged plasticity material model.

Compression properties of concrete were based on the Concrete Damage Plasticity (CDP) model of Abaqus. Concrete compressive strength was 34.5 MPa (5 ksi). The elastic modulus was calculated as per ACI 318 (2014). Inelastic concrete compressive behavior and tension properties of concrete were as described by FIB Model Code 2010 (FIB 2010). Mild steel was defined as

bilinear inelastic. The elastic modulus, yield stress, and ultimate stress were taken from ASTM A615/A615M (ASTM 2014) as 200000 MPa, 413.7 Mpa, and 620.5 Mpa (29,000 ksi, 60 ksi, and 90 ksi) respectively. For the inelastic response, isotropic hardening with a ratio of inelastic-to-elastic stiffness of 2% was used. A nonlinear stress-strain curve for post-tensioning strands in tension was defined per PCI design handbook (PCI 2010). Strands were 1861.6 MPa (270 ksi) ultimate strength, 15.2-mm (0.6-in.) diameter.

Results

Shear Wall with Non-Interlocking Tessellations

Fig 8 presents the load-displacement curve for the shear wall with non-interlocking tessellations.

The figure shows that a stable yield plateau can be reached. Redundancy of the wall and redistribution of load among tiles provided the displacement capacity.



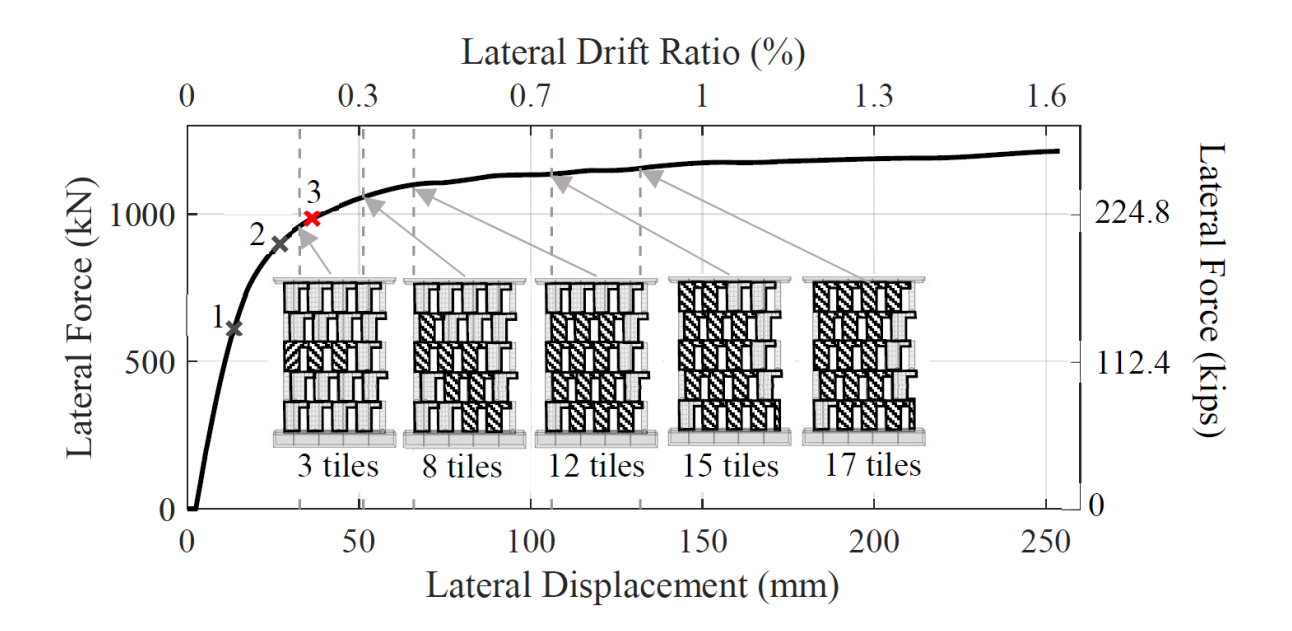


Fig. 8. Load-displacement behavior of the non-interlocking wall highlighting failure progression

316

317

318

319

320

321

322

323

324

325

326

327

328

329

330

331

332

333

334

335

336

337

Fig 8 also marks critical displacement levels as points 1 to 3. First gap opening between tiles (point 1) occur at displacement around 0.1% drift. Before gap opening, the wall remains effectively linear elastic. Gap opening is a recoverable displacement, as gaps are expected to close due to the restoring forces created by post-tensioning. Yet, it can provide nonlinearity to the system (between points 1 and 2). After point 2, individual tiles start reaching their compression capacity. After point 3, connectors between wall tiles start yielding. It should be noted that if connectors are built external to the walls, they can act as replaceable fuses such that they fail before the tiles. None of the post-tensioning strands yielded throughout the analysis. The tiles that exceed their compression capacity with increasing displacements are also marked in Fig 8. for several displacement levels. In this study, exceeding the compression capacity is defined as the criterion for individual tile failure. Failure modes (concrete crushing or reinforcement yielding) and locations can be controlled through changes in tile and connection design. The number of failed tiles will be a function of the displacement demand of an extreme event. As was demonstrated in the proof of concept physical experiment, it is conceivable that failed tiles can be replaced to restore stiffness and strength of the system without the need to replace the entire wall. The principal compression strain contour plot at the maximum displacement, 1.7% drift, is also shown in Fig 9. In this figure, strains higher than 0.3% were defined as compression failure. Most tile failures initiated in the horizontal portion of the L-shape. Prefabricating L-tiles in two pieces, horizontal (fuse element) and vertical, could further improve reparability by focusing damage on the relatively weak and potentially easier-to-replace horizontal pieces.

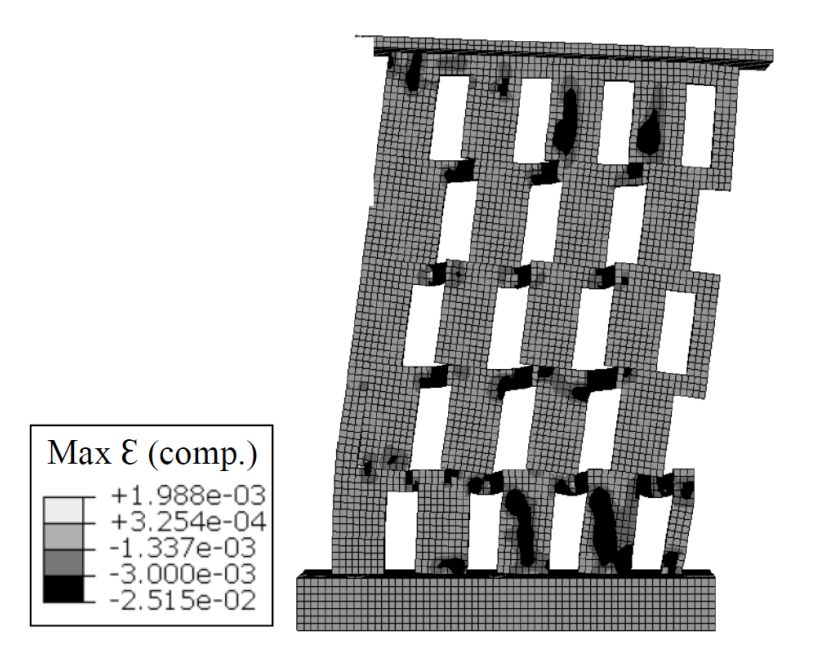


Fig. 9. Principal compression strains of the non-interlocking wall at 1.7% drift.

Shear Wall with Topologically-Interlocking Tessellations

The lateral load-displacement curve of the topologically-interlocking wall is given in Fig 10. Similar to the non-interlocking wall, the topologically-interlocking wall had a stable yield plateau. Unlike the non-interlocking wall, for the topologically-interlocking wall, this was accomplished without any mechanical connectors or post-tensioning between tiles. Displacement at which first concrete cracking occurred is marked as point 1 in Fig 10. Gap opening occurred immediately after lateral loading starts, since the self-weight of the wall is the only source considered for the initial contact. The nonlinearity in the load displacement is the result of recoverable gap opening between tiles and, to a lesser extent, material nonlinearity. This figure also highlights the tiles that reached concrete compressive strength with increasing drift ratios. These tiles can conceivably be replaced after an extreme event to keep the structure operational. Fig 11 shows the principal compressive strains at 1.7% drift ratio on the displaced shape for the topologically-interlocking wall. Finite elements that exceed their compressive strength are

highlighted. This figure shows that for some tiles, the damage is local which may allow repairing individual tiles, before a tile replacement is necessary.

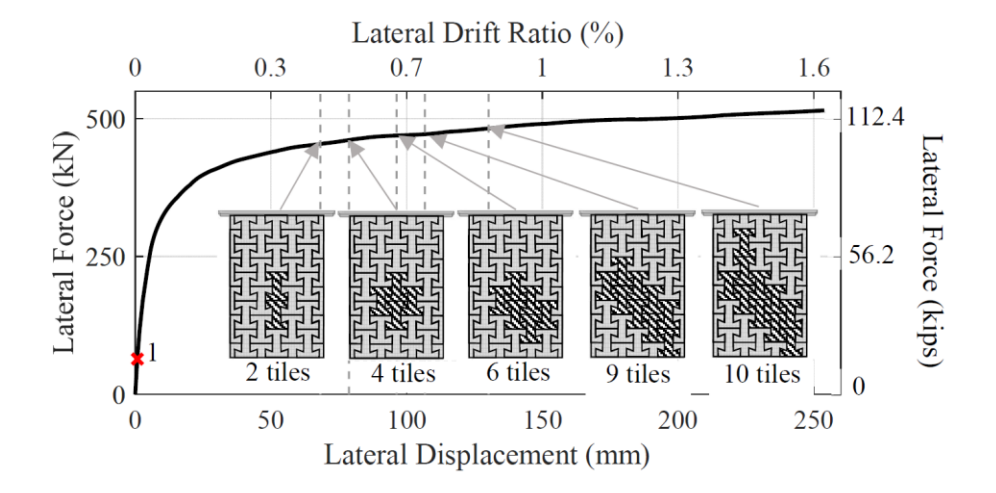


Fig. 10. Load-displacement behavior of the 2D interlocking wall highlighting failure progression.

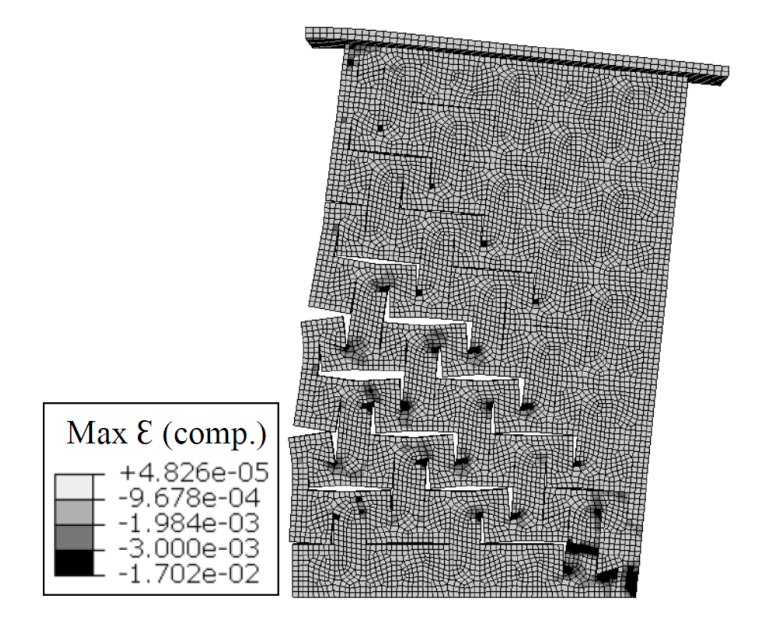


Fig. 11. Principal compression strains of the 2D interlocking wall at 1.7% drift.

In summary, preliminary analyses show that walls with non-interlocking and topologically-interlocking tessellations had the ductility and redundancy required from lateral load resisting elements. The walls were stable in the nonlinear range, indicating alternate load paths were available. Damage was contained to individual tiles, failures of which were gradual. This unique feature of tessellated walls allows replacement or repair of damaged tiles after extreme loading, enabling resiliency and sustainability.

Recommended steps towards implementation of TeSA

Implementation of TeSA systems will require research and development that is well beyond the scope of this paper. The paragraphs below briefly describe some practical hurdles that must be addressed prior to implementation. These hurdles were in-part identified through discussions between the authors and potential early adopters:

Connection tolerances. The nature of tessellation patterns demands well-fitted tiles. Small tolerance inaccuracies can propagate through an entire tessellation pattern. Thus, tiles in TeSA systems will need to be fabricated to tolerances that facilitate assembly, load transfer, and disassembly. Tile-to-tile details will need to be developed that allow for transfer of forces while also accounting for subtle variations in tile geometry that are beyond the tolerance controls of the fabrication process. Additionally, TeSA-to-floor connection details will need to be developed that facilitate force transfer while also bracing the TeSA walls in the out-of-plane direction.

Deconstruction and repair sequences. While removal and replacement of damaged tiles is theoretically appealing, it will be challenging to remove tiles that are supporting dead loads.

Shoring sequences will need to be developed that support the structure while the damaged tile is

replaced. Additionally, connection details will need to facilitate removal and replacement.

Thermal and vapor barriers. If TeSA walls are used on the outside of buildings, then interaction with the building envelope must be considered. One plausible option is to separate the thermal and vapor barriers from the TeSA system similar to brick veneer cavity wall assemblies (i.e. rain-screens). This option will require structural connections that transmit loads across the cavity and thermal barrier while also minimizing thermal bridging and opportunities for water intrusion. A better option will be to integrate the thermal and water barriers into the system, but this requires additional research and testing. Validation of structural models. The analyses presented in this paper are based on common practices for nonlinear structural modeling. Validation of the models is required prior to using the models for design. Characterization of Failure Criterion. The criterion for individual tile failure needs to be defined considering different types and levels of damage, including concrete cracking, crushing, and reinforcement yielding. Out-of-plane Performance. Out-of-plane behavior is out of this manuscript's scope, and will be investigated after developing a good understanding on the in-plane behavior. Possible methods to limit out-of-plane displacements include through-thickness interlocking or vertical frames that can carry out of plane loads. **Summary and Conclusions** A conceptual description of a tessellated structural-architectural (TeSA) system has been presented. The system features shear walls comprised of tessellated patterns built of individual tile elements. The concept was explored through a physical demonstration, nonlinear finite

386

387

388

389

390

391

392

393

394

395

396

397

398

399

400

401

402

403

404

405

406

407

element analyses, and through discussions with potential early adopters.

The TeSA system has many potential benefits. They are built by combining identical tiles into complex architectural patterns. As such, TeSA systems can be aesthetically interesting while also being well-suited to prefabrication, automated construction, reconfiguration, disassembly, and reuse. The system also has potential resilience and sustainability benefits. During extreme loading events TeSA systems can have localized damage to individual tiles while simultaneously providing alternate and ductile load paths. Damaged tiles can potentially be repaired or replaced, allowing TeSA buildings to be quickly reoccupied after the hazard event. The proof of concept physical experiment in this paper involved load testing of a small tessellated beam which was built from 2D interlocking acrylic tiles. The beam was simply supported and was tested under displacement-control until collapse. Damage associated with collapse was concentrated in two tiles, while the remaining tiles were unaffected during the test. Following collapse, the damaged tiles were replaced and the beam was tested again. The repaired beam had strength and stiffness that was effectively identical to the beam in its original state. Two types of TeSA shear walls were modeled analytically: non-interlocking tiles connected together with mechanical connectors and post-tensioning, and topologically-interlocking tiles with no mechanical connectors or post-tensioning. Finite element analyses showed that both walls had stable responses up to 1.7% lateral drift under monotonically increasing lateral displacements. Nonlinearity in lateral load-displacement response was due to the combined effects of concrete cracking, reinforcement or mechanical connector yielding, and gap opening. The latter is a recoverable displacement upon unloading. Both walls had gradual failure of individual tiles in succession, leading to a redundant and ductile response. It is conceivable that failed tiles could be replaced or repaired for a fast recovery from extreme event.

408

409

410

411

412

413

414

415

416

417

418

419

420

421

422

423

424

425

426

427

428

429

While the concept is promising, further research and development is required to actualize TeSA systems in buildings. Further work is recommended on practical issues such as tolerance and detailing, construction and deconstruction sequencing, and vapor and thermal barriers when the TeSA system interacts with the building envelope. Work is also needed to validate structural models for TeSA systems. The aesthetic and structural benefits of TeSA systems are considered sufficient to invest effort in the development of practical solutions. Acknowledgements This material is based upon work supported by the National Science Foundation under Grants No. 1762899 and 1762133. Any opinions, findings, and conclusions or recommendations expressed in this material are those of the authors and do not necessarily reflect the views of the National Science Foundation. The authors also acknowledge and thank Sachin Sreedhara and Vishnu Sreenath for their assistance in the physical experiment described in the paper, and Sida Dai for his contributions towards illustrations and figures. **Data Availability Statement** Some or all data, models, or code that support the findings of this study are available from the corresponding author upon reasonable request. Available data include output files from the finite element analyses. References ACI (American Concrete Institute). 2014. Building code requirement for reinforced concrete. ACI 318-14. Farmington Hills, MI: ACI. Adami, D. 2012. "Tessellation (Image modified from the original)." Accessed September 1, 2017. https://flic.kr/p/bdPnCD. Available for use under license:

431

432

433

434

435

436

437

438

439

440

441

442

443

444

445

446

447

448 449

450

451

452

453

454

https://creativecommons.org/licenses/.

- 455 by-sa/2.0/legalcode.>
- 456 ASTM (American Society for Testing and Materials International) ASTM A615 / A615M. 2009.
- 457 Standard Specification for Deformed and Plain Carbon-Steel Bars for Concrete Reinforcement.
- 458 West Conshohocken, PA: ASTM.
- 459 Brugger, C., Fivel, M. C., and Bréchet, Y. 2009. "Numerical Simulations of Topologically
- 460 Interlocked Materials Coupling DEM Methods and FEM Calculations: Comparison with
- 461 Indentation Experiments." MRS Proc., Symposium LL—Architectured Multifunctional
- 462 Materials, 1188, LL05-05, https://doi.org/10.1557/PROC-1188-LL05-05.
- Chavey, D. 1989. "Tilings by regular polygons—II: A catalog of tilings." Comput. Math. Appl.,
- 464 17 (1–3), 147-165.
- 465 Critchlow, K. 1970. Order in Space: A Design Source Book. Viking Press, New York, 120.
- Dassault Systèmes Simulia Corporation. 2016. ABAQUS 6.16-1. 6.16 ed, Providence, RI.
- 467 https://www.3ds.com/products-services/simulia/products/abaqus/
- Dunlop, J. W. C., and Brechet, Y. J. M. 2009. "Architectured structural materials: A parallel
- between nature and engineering." MRS Proc., Symposium LL—Architectured Multifunctional
- 470 Materials, 1188, LL09-04. https://doi.org/10.1557/PROC-1188-LL09-04
- Epsilon, S. 2013. "Al Bahar Towers Responsive Facade." Accessed September 1, 2017.
- https://flic.kr/p/ezQiGU. Available for use under license:
- 473 https://creativecommons.org/licenses/by-sa/2.0/legalcode.
- Estrin, Y., Dyskin, A. V., Pasternak, E., Schaare, S., Stanchits, S., and Kanel-Belov, A. J. 2004.
- "Negative stiffness of a layer with topologically interlocked elements." Scr. Mater., 50(2), 291-
- 476 294. https://doi.org/10.1016/j.scriptamat.2003.09.053.

- 477 Evanson, T. 2013. "Kogod Courtyard looking west and up Smithsonian American Art
- 478 Museum (modified from the original)." Accessed September 1, 2017.
- https://flic.kr/p/dHH8pD. Available for use under license:
- 480 https://creativecommons.org/licenses/by-sa/2.0/legalcode.
- 481 fee-ach 2006. "L'Institut du monde arabe (image modified from the original)." Accessed
- 482 September 1, 2017.
- 483 https://flic.kr/p/HkYhZs. Available for use under license:
- https://creativecommons.org/licenses/by-sa/2.0/legalcode.
- 485 FIB (Fédération Internationale du Béton). 2010. fib model code for concrete structures 2010,
- 486 Lausanne, Switzerland: FIB.
- Fleury, F. 2009. "Evaluation of the perpendicular flat vault inventor's intuitions through large
- scale instrumented testing." *Proc. Third Int. Congress on Construction History*, 611-618. BTU
- 489 Cottbus, Cottbus, Germany.
- 490 Glickman, M. 1984. "The G-Block system of vertically interlocking paving" *Proc., 2nd Int Conf*
- 491 *on ConcreBlock Paving*, 345-348, Delft, Netherlands.
- Khandelwal, S. 2013. "Hybrid and smart topologically interlocking materials." Ph.D.
- 493 Dissertation, Purdue University, West Lafayette, IN.
- Knight, T. W. 1986. "Transformations of the meander motif on Greek geometric pottery."
- 495 *Design Computing*, 1(1), 29-67.
- 496 Knight, T. W. 1995. Transformations in design: a formal approach to stylistic change and
- 497 *innovation in the visual arts.* Cambridge, England: Cambridge University Press.

- 498 Krauss, S., Monsonego-Ornan, E., Zelzer, E., Fratzl, P., and Shahar, R. 2009. "Mechanical
- 499 function of a complex three-dimensional suture joining the bony elements in the shell of the red-
- eared slider turtle." *Adv. Mater.*, 21(4), 407-412. https://doi.org/10.1002/adma.200801256.
- Magnus, W. 1974. Non-euclidean tessellations and their groups, Pure and applied mathematics.
- 502 New York: Academic Press,
- Manning, L. 2009. "290 Mulberry St (image modified from the original)." Accessed September
- 1, 2017. https://flic.kr/p/6UTqAN. Available for use under license:
- 505 https://creativecommons.org/licenses/by-sa/2.0/legalcode.
- Mather, A., Cipra, R., and Siegmund, T. 2012. "Structural integrity during remanufacture of a
- topologically interlocked material." *Int J. of Struct. Integ.*, 3(1), 61-78.
- 508 https://doi.org/10.1108/17579861211210009.
- Molotnikov, A., Estrin, Y., Dyskin, A. V., Pasternak, E., and Kanel-Belov, A. J. 2007.
- 510 "Percolation mechanism of failure of a planar assembly of interlocked osteomorphic elements."
- 511 Eng. Fract Mech., 74(8), 1222-1232. https://doi.org/10.1016/j.engfracmech.2006.07.012.
- Moon, K.-S., Connor, J. J., and Fernandez, J. E. 2007. "Diagrid structural systems for tall
- buildings: characteristics and methodology for preliminary design." Struct. Des. Tall. Special
- 514 *Build.*, 16(2), 205-230. https://doi.org/10.1002/tal.311.
- Moore, D. 1995a. "The Pantheon." Accessed September 1, 2017.
- 516 http://www.romanconcrete.com/docs/chapt01/chapt01.htm.
- Moore, D. 1995b. *The Roman Pantheon: the triumph of concrete*. Guam: MARC/CCEOP,
- 518 University of Guam Station.
- Perry, W., Broers, A., El-Baz, F., Harris, W., Healy, B., and Hillis, W. 2008. "Grand Challenges
- for Engineering." Updated 2017, National Academy of Engineering. Washington, DC, 52.

- 521 PCI (Precast/Prestressed Concrete Institute). 2010. PCI design handbook, (7th Ed.), Chicago, IL:
- 522 PCI.

- Rezaee Javan, A., Seifi, H., Xu, S., Ruan, D., and Xie, Y. M. 2017. "The impact behaviour of
- 524 plate-like assemblies made of new interlocking bricks: An experimental study." *Mater. Design.*,
- 525 134, 361-373, https://doi.org/10.1016/j.matdes.2017.08.056.
- 526 Schaare, S., Dyskin, A. V., Estrin, Y., Arndt, S., Pasternak, E., and Kanel-Belov, A. 2008. "Point
- loading of assemblies of interlocked cube-shaped elements." Int. J. Eng. Sci., 46(12), 1228-1238,
- 528 http://dx.doi.org/10.1016/j.ijengsci.2008.06.012.
- 529 SHoP Architects. n.d. "Mulberry House." Accessed September 1, 2017.
- 530 http://www.shoparc.com/projects/mulberry-house/.
- 531 Shubnikov, A., Koptsik, V. (Ed.). 1974. Symmetry in science and art. New York: Springer.
- 532 Steve, L. 2012. "Gherkin: London (Image modified from the original)." Accessed September 1,
- 533 2017. https://flic.kr/p/bKX6E6. Available for use under license:
- https://creativecommons.org/licenses/by-sa/2.0/legalcode.
- Zareiyan, B., and Khoshnevis, B. 2017. "Effects of interlocking on interlayer adhesion and
- strength of structures in 3D printing of concrete." *Automat. Constr.* 83, 212-221,
- 537 https://doi.org/10.1016/j.autcon.2017.08.019.